Kinetic and Thermodynamic Framework for Assembly of the Six-Component bI3 Group I Intron Ribonucleoprotein Catalyst†

Gurminder S. Bassi‡ and Kevin M. Weeks*

Department of Chemistry, University of North Carolina, Chapel Hill, North Carolina 27599-3290

Received April 29, 2003; Revised Manuscript Received June 9, 2003

ABSTRACT: The yeast mitochondrial bI3 group I intron RNA splices in vitro as a six-component ribonucleoprotein complex with the bI3 maturase and Mrs1 proteins. We report a comprehensive framework for assembly of the catalytically active bI3 ribonucleoprotein. (1) In the absence of Mg^{2+}, two Mrs1 dimers bind independently to the bI3 RNA. The ratio of dissociation to association rate constants, k_{off}/k_{on}, is approximately equal to the observed equilibrium $K_{1/2}$ of 0.12 nM. (2) At magnesium ion concentrations optimal for splicing (20 mM), two Mrs1 dimers bind with strong cooperativity to the bI3 RNA. k_{off}/k_{on} is 15-fold lower than the observed $K_{1/2}$ of 11 nM, which reflects formation of an obligate intermediate involving one Mrs1 dimer and the RNA in cooperative assembly of the Mrs1−RNA complex. (3) The bI3 maturase monomer binds to the bI3 RNA at almost the diffusion-controlled limit and dissociates with a half-life of 1 h. k_{off}/k_{on} is approximately equal to the equilibrium K_D of 2.8 pM. The bI3 maturase thus represents a rare example of a group I intron protein cofactor whose binding is adequately characterized by a one-step mechanism under conditions that promote splicing. (4) Maturase and Mrs1 proteins each bind the bI3 RNA tightly, but with only modest coupling (∼1 kcal/mol), suggesting that the proteins interact at independent RNA binding sites. Maturase binding functions to slow dissociation of Mrs1; whereas prior Mrs1 binding increases the bI3 maturase k_{on} right to the diffusion limit. (5) At effective concentrations plausibly present in yeast mitochondria, a predominant assembly pathway emerges involving rapid, tight binding by the bI3 maturase, followed by slower, cooperative assembly of two Mrs1 dimers. In the absence of other factors, disassembly of all protein subunits will occur in a single apparent step, governed by dissociation of the bI3 maturase.

RNA-based active sites carry out many of the reactions most fundamental to biology (*1*). However, most contemporary RNA-based reactions are dependent on protein cofactors to achieve their functional structure and for a myriad of other functions. Our laboratory has begun to take a comparative ribonucleoprotein analysis approach to understand the molecular mechanisms by which RNA and proteins collaborate to optimize the functioning of RNA active sites (*2*, *3*).

Studies of protein-facilitated catalysis by complexes containing group I intron RNAs are especially instructive for understanding ribonucleoprotein assembly reactions because acquisition of the native, functional state is reported directly by splicing. Group I introns fold into a well-defined three-dimensional structure (*4*, *5*), which binds a guanosine nucleophile cofactor and, in turn, the 5′ and 3′ splice sites (*6*). Splicing occurs via successive transesterification reactions to yield ligated exons and the excised intron covalently linked to a 5′ guanosine (Scheme 1). Most group I introns, like cellular RNAs generally, require binding by one or more protein cofactors to achieve a catalytically active structure.

Scheme 1

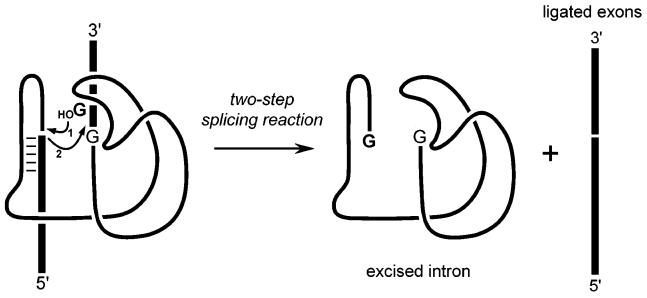

In vitro studies of protein-facilitated splicing of group I introns have emphasized that diverse protein cofactors play related roles and function to stabilize the catalytically active state of an RNA. CBP2 is a monomeric protein that recognizes idiosyncratic features of the *S. cerevisiae* bI5 group I intron (*2*, *7*, *8*). CYT-18, a dimeric tRNA synthetase, stabilizes the group I intron P5-P4-P6 RNA domain in the *N. crassa* LSU intron and in other group I introns in which this domain is accessible (*2*, *9*, *10*). The AnCob maturase is a monomeric protein, apparently evolved from a preexisting family of double-stranded DNA endonucleases, that facilitates splicing of the third group I intron in the cytochrome *b* gene of *A. nidulans* (*11*−*13*). Strikingly, even in cases where two protein cofactors appear to stabilize the same active RNA state, the molecular mechanisms underlying

† This work was supported by a grant from the N.I.H. (GM56222 to K.M.W.) and by a Human Frontiers Science Program Long-Term Fellowship to G.S.B.

* Corresponding author. E-mail: weeks@unc.edu.

‡ Present address: Centre de Génétique Moléculaire−Bât. 26, CNRS 91198 Gif-sur-Yvette, Cedex, France.

10.1021/bi0346906 CCC: $25.00
Published on Web 07/30/2003

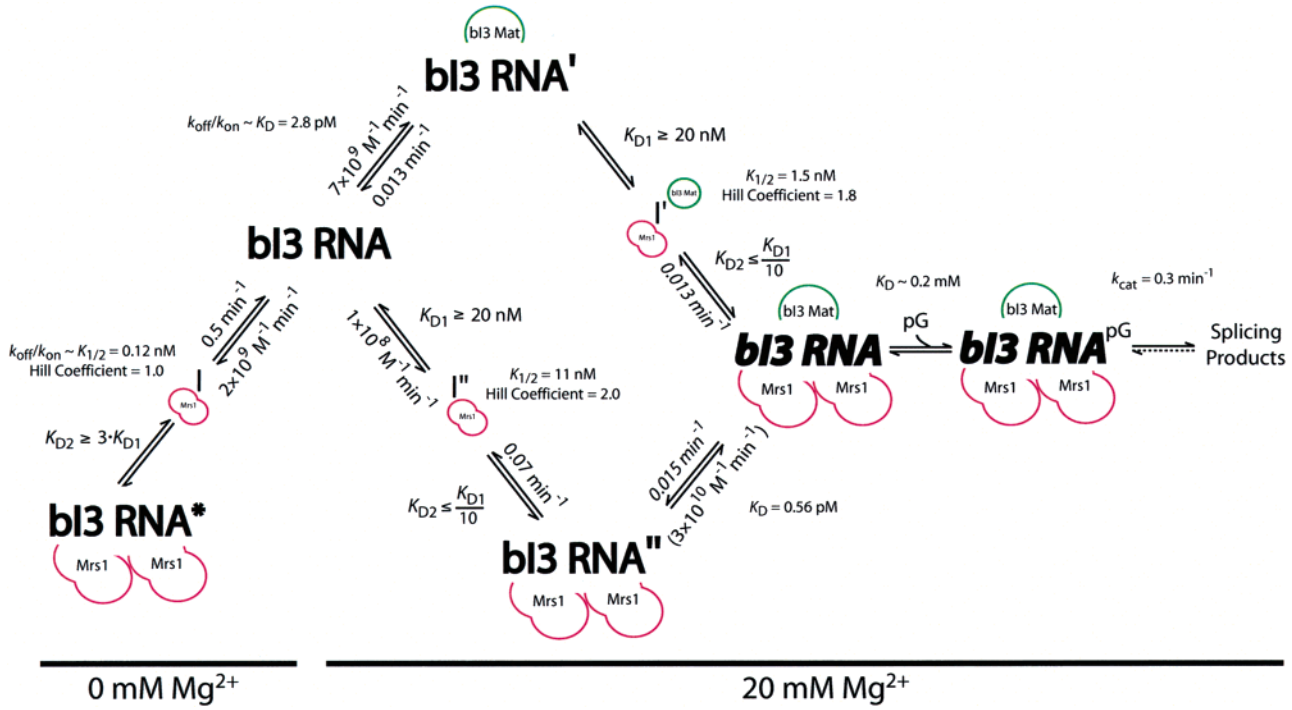

FIGURE 1: Assembly of and splicing by the bI3 group I intron ribonucleoprotein catalyst. bI3 RNA*, bI3 RNA′, and bI3 RNA″ are structurally distinct, partially assembled, states for the bI3 group I intron. The catalytically active RNA is shown in bold. I_{Mrs1} is an RNA intermediate with a single bound Mrs1 dimer, and pG is the guanosine 5′-monophosphate nucleophile. The rate constant for association of maturase with the Mrs1-RNA complex is calculated from other values and is therefore shown in parentheses. Rate constants for dissociation of maturase and Mrs1 from the holocomplex are taken as the rate of dissociation from the holocomplex post splicing and are shown in italics.

productive ribonucleoprotein assembly can be completely different (*2*).

These one protein−one RNA systems, however, lack the feature most characteristic of more prominent ribonucleoproteins, like the spliceosome or ribosome, that of functional coupling between multiple protein components. In an effort to develop a deeper understanding of assembly and catalysis in large ribonucleoprotein complexes, we are exploring protein-facilitated splicing for the *S. cerevisiae* cytochrome *b* bI3 group I intron.

The bI3 group I intron RNA requires both an intron encoded protein, the bI3 maturase, and a nuclear encoded protein, Mrs1, for efficient splicing in vitro (*3*). The evolutionary origin of each protein is distinct. The bI3 maturase is translated in frame with the first two cytochrome *b* exons (*14*). The intron encoded segment of the protein contains two domains (*3*), a hydrophobic, possibly membrane bound, domain, and a LAGLIDADG-motif domain, conserved in a large family of DNA endonucleases and RNA maturases (*15*). The soluble LAGLIDADG domain is sufficient for RNA binding and splicing facilitation functions (*3*, *16*). Mrs1 is a highly diverged member of a family of dimeric DNA resolvases, most of whose members bind and cleave four-way junctions (*17*).

Thus, both the bI3 maturase and the Mrs1 proteins, which now function in RNA splicing, appear to have evolved from preexisting DNA-binding functions. Both proteins have evolved to the extent that they have lost or are severely compromised in the DNA cleavage activities characteristic of their closest homologues (reviewed in ref *3*).

The bI3 maturase binds the RNA as a monomer, whereas two Mrs1 dimers bind with strong cooperativity to the bI3 RNA under optimal splicing conditions. The six-subunit bI3 ribonucleoprotein has an approximate mass of 420 kDa. At saturating guanosine substrate, the complex splices with a k_{cat} of 0.3 min^{-1}, which represents at least a 10^4-fold acceleration over splicing by the RNA alone (*3*).

We outline a comprehensive kinetic and thermodynamic framework for assembly of the six-component bI3 ribonucleoprotein catalyst (Figure 1). Analysis of the resulting framework permits characterization of obligate assembly intermediates, intersubunit cooperative interactions, and predominant assembly pathways for this large ribonucleoprotein. This assembly framework for the bI3 ribonucleoprotein catalyst also illustrates principles important for future investigations directed toward understanding protein modulation of RNA active sites in this and other systems.

EXPERIMENTAL PROCEDURES

Proteins and bI3 RNA. $(His)_{10}$-tagged Mrs1 and bI3 maturase proteins were purified by affinity chromatography on a Ni^{2+}-NTA resin (Qiagen, Chatsworth, CA) (*3*). Concentrations of the purified proteins were obtained from their molar absorptivities (*18*). Mrs1 is a solution dimer (*3*), and concentrations of this protein are therefore reported in terms of the functional dimer. The bI3-ΔL8 RNA, lacking an ∼1300 nucleotide open reading frame, was generated by runoff transcription from linearized plasmid DNA templates and purified by denaturing gel electrophoresis (*3*). The bI3-ΔL8 RNA, or for simplicity, bI3 RNA precursor spanned 85 nt of the 5′ exon, the 488 nt simplified intron, and a 31 nt 3′ exon. All experiments were carried out at 36 °C in reaction buffer containing 40 mM Hepes (pH 7.5), 80 mM potassium-acetate (pH 7.4), 0 or 20 mM $MgCl_2$, 1 mM DTT, and 10 μg/mL BSA. To renature purified RNA, precursor

RNA was heated to 90 °C for 1 min, placed on ice, and incubated at 36 °C for 10 min in reaction buffer.

Error Analysis. All equilibrium and rate measurements were repeated 2−4 times, and errors are reported conservatively to encompass the full range of data obtained rather than as the smaller standard deviation value.

Equilibrium Binding and Complex Association and Dissociation. Filter partitioning experiments were performed using nitrocellulose and positively charged filters to capture both protein-bound and free RNAs, as described (*3*, *7*). In exploratory experiments, observed dissociation constants for maturase and Mrs1 were identical for equilibration periods of 1 and 10 h, indicating that 1 h is sufficient to achieve equilibrium; a 1 h equilibration was used for subsequent measurements. To determine individual complex assembly rates, reactions were initiated by adding either bI3 maturase or Mrs1 to 10 pM ^{32}P-labeled bI3 RNA. Binding was quenched with excess (400−1000-fold) bI3 RNA, and aliquots were immediately filtered on the double filter partitioning system. Rates were obtained by fitting the fraction bound to an equation describing a single exponential, fraction RNA bound $= A(1 - e^{-kt})$, where k is the observed rate, and A is the fraction RNA bound at long time points. In all cases, control experiments in which unlabeled RNA was added prior to protein showed that the quench quantitatively eliminated additional protein binding. Second-order association rate constants (k_{on}) were obtained from linear fits of observed rate versus protein concentration. For all experiments, RNAs were quantified using a Phosphorimager (Molecular Dynamics).

Complex dissociation rates (k_{off}) were measured using 100 pM ^{32}P-labeled bI3 RNA and (i) 0.5 or 1 nM bI3 maturase in 20 mM Mg^{2+}, (ii) 1 or 3 nM Mrs1 in 0 mM Mg^{2+}, or (iii) 40 nM Mrs1 in 20 mM Mg^{2+}. RNA−protein complexes were incubated at 36 °C for 45 min and then diluted into 20 or 80 μg/mL heparin to trap dissociating protein. Aliquots were filtered using the dual filter partitioning system, and dissociation rates were calculated by fitting fraction RNA bound to a single exponential.

Determining k_{off} for Individual Proteins in the Six-Subunit Complex. To monitor bI3 maturase turnover, 100 nM ^{32}P-labeled bI3 RNA was incubated with 250 nM Mrs1 and (limiting concentrations of) bI3 maturase at 3 or 5 nM. For Mrs1 turnover, 300 nM ^{32}P-labeled bI3 RNA was incubated with 400 nM bI3 maturase and 30 or 50 nM Mrs1. The fraction of spliced precursor (over 2−3 h) was normalized to account for the fraction RNA (typically 25%) that does not react at long time periods at saturating protein concentrations. The linear slope after the first turnover yields k_{off}[protein]/[RNA] (*19*).

Protein-Limited Splicing Assays to Determine Protein−Protein Coupling in the Six-Subunit Complex. The fraction RNA bound by a titrated protein in the holocomplex was determined as the fraction RNA competent for splicing at a time point where the first turnover of the holoenzyme was complete (40 min). Protein−RNA complexes were incubated for 1 h prior to initiating splicing. To determine the $K_{1/2}$ of Mrs1 for a preformed RNA-bI3 maturase complex, splicing reactions (20−25 μL) were performed with 100 pM ^{32}P-labeled bI3 RNA and 500 pM (saturating) bI3 maturase. Mrs1 concentrations were 0.25−32 nM. The K_D of the bI3 maturase for a preformed bI3 RNA−Mrs1 complex was determined in splicing reactions (1.5 mL) using 0.035 pM ^{32}P-labeled bI3 RNA and 10 nM (saturating) Mrs1. Reactions were quenched by addition of EDTA to 100 mM and precipitation with ethanol. bI3 maturase concentrations spanned 0.1−20 pM. Splicing reactions were resolved by 4% (w/v) polyacrylamide/7 M urea gels (see Figure 2 in ref *3*).

RESULTS

Preface. Splicing by the bI3 group I intron requires two proteins in vitro, the intron encoded bI3 maturase and a nuclear encoded protein, Mrs1 (Figure 1). Both proteins bind independently to the intron RNA. The bI3 maturase binds to the RNA as a monomer with an equilibrium dissociation constant, K_D, of 2.8 pM (*3*). Mrs1 is a solution dimer, and two Mrs1 dimers bind to the bI3 RNA in a strongly magnesium ion-dependent assembly reaction. In the absence of Mg^{2+}, two Mrs1 dimers bind noncooperatively to the bI3 RNA. The concentration at which one-half of the RNA is bound by Mrs1, the $K_{1/2}$, is 0.12 nM. Under conditions optimal for splicing (20 mM Mg^{2+}), assembly of two Mrs1 dimers with the bI3 RNA is strongly cooperative; the $K_{1/2}$ is 11 nM and the empirical Hill coefficient is 2.0 (*3*) (Figure 1).

The assembly mechanism developed in this work uses a standard state of 20 mM Mg^{2+}, where splicing is most efficient. Maturase binding and cooperative Mrs1 interactions with the bI3 RNA are substantially similar for all Mg^{2+} concentrations greater than 8 mM (data not shown). Thus, we anticipate that global features of this mechanism will apply over a broad range of ionic environments.

Assembly and Dissociation of the Maturase-bI3 RNA Complex. To monitor association of maturase with the bI3 RNA, pre-folded RNA was rapidly mixed with maturase, complex formation was quenched at intervals with excess pre-folded RNA, and bound and free RNAs were resolved by filter partitioning. Complex formation showed good pseudo-first-order behavior, and the observed association rate increased from 1.5 min^{-1} at 0.2 nM to 5.5 min^{-1} at 0.7 nM (Figure 2A). The association rate constant for formation of the bI3 maturase−RNA complex is equal to the slope of observed association rate as a function of protein concentration (Figure 2B). The association rate constant, k_{on} [7 ($\pm$ 4) $\times$ 10^9 M^{-1} min^{-1}], is within an order of magnitude of the diffusion-controlled limit (*20*).

Dissociation of preformed bI3 maturase−RNA complexes was monitored at two protein concentrations. Dissociating protein was trapped by the addition of heparin, which efficiently competes with reassembly of the complex. The fraction of bound complex, at 0.5 or 1 nM bI3 maturase, following heparin addition is well-fit by a single exponential. The dissociation rate constant, k_{off}, is 0.013 ($\pm$0.006) min^{-1}, corresponding to a half-life of ~1 h (Figure 2C). Slow dissociation is independently supported by the small y intercept seen in Figure 2B.

The ratio of k_{off} to k_{on} for the maturase−bI3 RNA complex is equal to (0.013 min^{-1})/(7 $\times$ 10^9 M^{-1} min^{-1}) or 1.9 pM. This value is in excellent agreement with the independently measured equilibrium dissociation constant of 2.8 pM (*3*). Thus, maturase assembly with the intron RNA is well-characterized as a simple one-step bimolecular process with

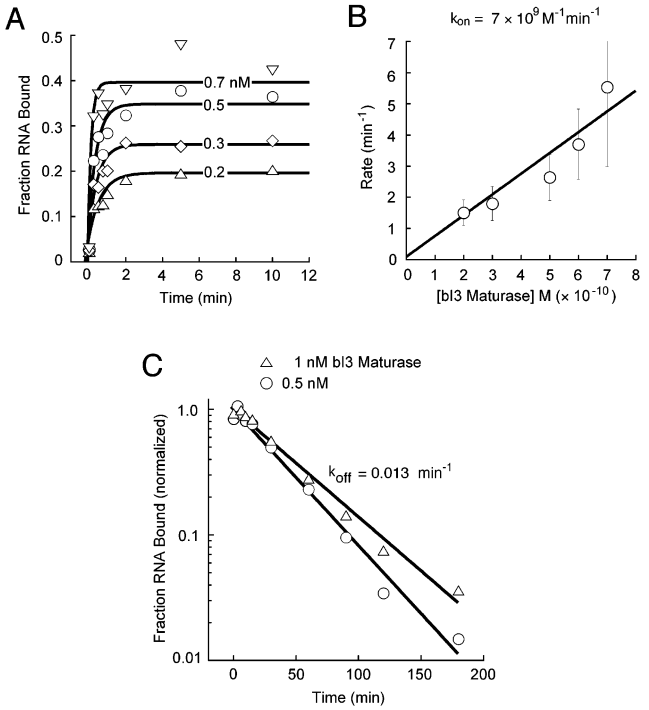

FIGURE 2: Assembly (k_{on}) and disassembly (k_{off}) of the maturase−bI3 RNA complex at 20 mM Mg^{2+}. (A) Assembly of the bI3 maturase−RNA complex monitored by filter partitioning at the indicated concentrations of bI3 maturase. (B) Pseudo-first-order rates obtained in individual binding experiments plotted as a function of protein concentration. The slope yields k_{on}. (C) Disassembly of either 0.5 nM (open circles) or 1 nM (open triangles) bI3 maturase-radiolabeled RNA complexes was initiated by addition of 20 μg/mL heparin and monitored by filter partitioning.

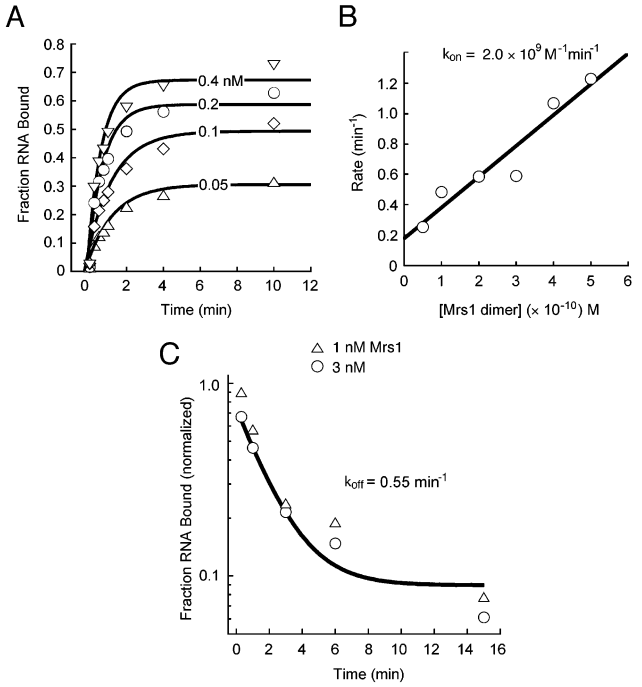

FIGURE 3: Assembly (k_{on}) and disassembly (k_{off}) of the Mrs1-bI3 RNA complex in the absence of Mg^{2+}. (A) Assembly of the Mrs1-bI3 RNA complex was monitored by filter partitioning at the indicated concentrations of Mrs1, and pseudo-first-order rates obtained in individual binding experiments are plotted as a function of protein concentration in panel B. (C) Dissociation of Mrs1 from preformed protein-radiolabeled RNA complexes was trapped with 20 μg/mL heparin and monitored by filter partitioning.

no kinetically significant intermediates (see maturase binding steps in Figure 1).

Noncooperative Assembly and Dissociation of the Mrs1-bI3 RNA Complex. We first monitored assembly of Mrs1 with the RNA in the absence of Mg^{2+}, where each of two Mrs1 dimers binds independently (*3*). The bI3 RNA was prefolded and rapidly mixed with Mrs1 dimer, and additional complex formation was quenched with excess prefolded RNA. Observed association rates increased from 0.6 min^{-1} at 0.05 nM to 1.3 min^{-1} at 0.4 nM (Figure 3A). The second-order association rate constant (k_{on}) for formation of the Mrs1−RNA complex is 2.0 (±0.3) × 10^9 M^{-1} min^{-1} (Figure 3B).

Dissociation of a preformed Mrs1-bI3 RNA complex at 0 mM Mg^{2+} was initiated by trapping dissociating protein with heparin (Figure 3C). The observed dissociation rate constant, k_{off}, is 0.55 (±0.2) min^{-1}. Thus, in the absence of Mg^{2+}, Mrs1−RNA complexes dissociate rapidly, with a half-life of 1.4 min.

The ratio, k_{off} to k_{on}, for the Mrs1-bI3 RNA complex at 0 mM Mg^{2+}, (0.55 min^{-1})/(2.0 × 10^9 M^{-1} min^{-1}) = 0.28 nM, is in good agreement with the equilibrium $K_{1/2}$ of 0.12 nM (*3*). These data suggest a mechanism in which the two Mrs1 dimers bind independently to the RNA, and each binding and dissociation event reflects a single kinetically significant step.

Cooperative Assembly and Dissociation of the Mrs1-bI3 RNA Complex. At Mg^{2+} concentrations of 8 mM and above, binding by two Mrs1 dimers is strongly cooperative. We monitored assembly and disassembly of Mrs1−RNA complexes at 20 mM Mg^{2+}, where splicing is efficient and nonspecific protein binding is suppressed (*3*). A plot of observed association rate (Figure 4A) as a function of Mrs1 dimer concentration yielded a good linear relationship (Figure 4B). The association rate constant [1.1 (±0.2) × 10^8 M^{-1} min^{-1}] is an order of magnitude slower than obtained in the absence of Mg^{2+} (compare Figures 3B and 4B).

The dissociation rate constant was determined in a heparin trapping experiment (Figure 4C) to be 0.07 (±0.02) min^{-1}, corresponding to a half-life of 10 min. Thus, relative to Mrs1 assembly observed in the absence of Mg^{2+}, at 20 mM Mg^{2+} the complex dissociates 6-fold more slowly.

The ratio of k_{off} to k_{on} for the Mrs1-bI3 RNA complex at 20 mM Mg^{2+} (0.07 min^{-1})/(1.1 × 10^8 M^{-1}min^{-1}) is 0.6 nM. This ratio differs from the equilibrium $K_{1/2}$ by 15-fold, a difference greater than the experimental uncertainty in our rate measurements.

Disagreement between association and dissociation rate constants, measured in a partitioning experiment, and the equilibrium K_D represents one kinetic signature for formation of an obligate intermediate in a macromolecular assembly reaction (*21*). The requirement for an obligate intermediate is not surprising in this case as, at a minimum, strongly cooperative binding by Mrs1 dimers implies an intermediate state in which a single Mrs1 dimer is bound to the bI3 RNA. Formation of this one Mrs1 dimer−one RNA complex creates a new interface with increased affinity for the second Mrs1 dimer (see Mrs1 assembly steps for 20 mM Mg^{2+} in Figure 1).

Multiple Turnover Kinetics to Determine k_{off} for Individual Proteins in the Six-Component Complex. Dissociation of both

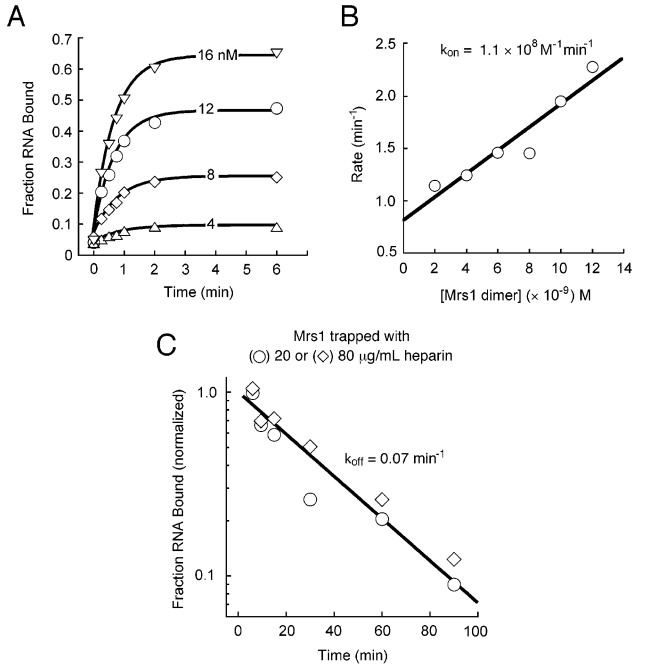

FIGURE 4: Assembly (k_{on}) and disassembly (k_{off}) of the Mrs1-bI3 RNA complex at 20 mM Mg^{2+}. Assembly of the Mrs1-bI3 RNA complex was monitored at the indicated concentrations of Mrs1 (A), and the second-order association rate constant was obtained from the slope shown in panel B. (C) Disassembly of a 40 nM Mrs1-radiolabeled bI3 RNA complex was initiated by addition of 20 (open circles) or 80 (open diamonds) μg/mL heparin and monitored by filter partitioning. Addition of heparin prior to protein eliminates coretention of the RNA on the nitrocellulose filter (not shown).

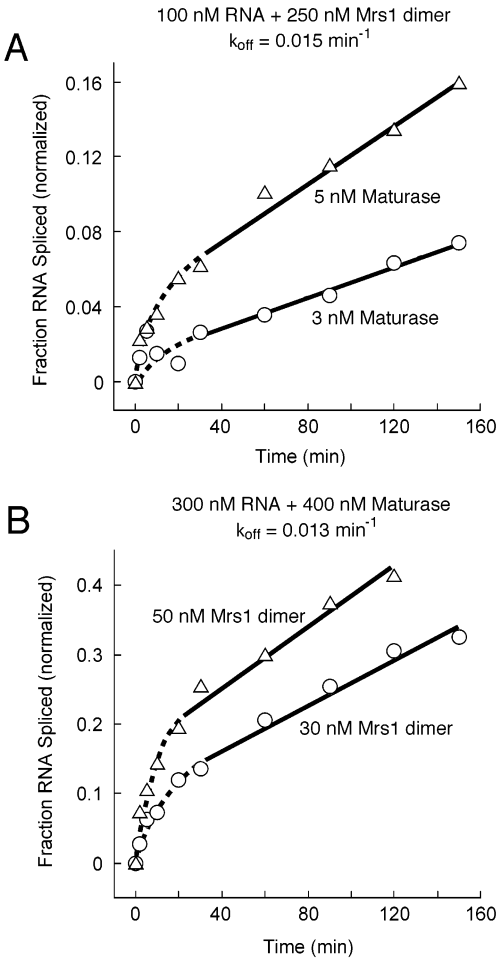

FIGURE 5: Disassembly of the bI3 maturase (A) and Mrs1 (B) from the six-subunit complex, monitored in multiple turnover splicing assays using excess RNA. The first turnover and multiple turnover phases are shown as dashed and solid lines, respectively. The slope of the multiple turnover phase is equal to k_{off}[protein]/[RNA]. The fraction spliced RNA precursor was normalized to the fraction of active RNA, equal to 75%.

maturase and Mrs1 is much slower (Figures 2C and 4C) than the rate of splicing (0.3 min^{-1} (*3*)) at 20 mM $MgCl_2$. If dissociation remains slow in the holocomplex, rate-limiting dissociation of a protein cofactor can be measured by following the multiple turnover phase of a splicing assay performed with excess RNA. The initial burst, corresponding to the first splicing event, will reflect the stoichiometry of protein binding. The subsequent linear phase is proportional to the rate constant, k_{off}, for dissociation from the catalytically competent RNA by the limiting protein.

Experiments show this is indeed the case. For example, 100 nM bI3 RNA and excess (250 nM) Mrs1 dimer were incubated with (limiting) 3 or 5 nM bI3 maturase, conditions where all components are present at concentrations above their K_D or $K_{1/2}$ in the holocomplex. There is an initial burst (dashed lines in Figure 5A) whose amplitude is approximately equivalent to the fraction RNA that forms a complete six-subunit holoribonucleoprotein. The fraction spliced after this first turnover (solid lines in Figure 5A), at both 3 and 5 nM maturase, yields a steady-state turnover rate constant, equal to k_{off}, of 0.015 ($\pm$0.002) min^{-1} (Figure 5A). k_{off} for the bI3 maturase in the holocomplex is identical, within error, to the k_{off} for its complex with the RNA alone (compare Figures 2C and 5A).

Comparable multiple turnover experiments were performed to measure rate-limiting dissociation of Mrs1 dimers at 30 and 50 nM from the six-subunit complex. The dissociation rate constant, k_{off}, is 0.013 ($\pm$0.002) min^{-1} (solid lines in Figure 5B). Thus, Mrs1 dimers dissociate 5-fold more slowly from the six-subunit complex than from the bI3 RNA alone (compare Figures 4C and 5B).

Interprotein Coupling in the bI3 Holoribonucleoprotein. Detectable splicing by the bI3 intron RNA is absolutely dependent on both maturase and Mrs1 proteins (*3*). Dissociation of either protein, independently (Figures 2 and 4) or in the six-subunit complex (Figure 5), is slow relative to the rate of splicing (0.3 min^{-1}). Given these constraints, the fraction RNA bound by both proteins can be measured in a straightforward way as the fraction RNA in a maturase-Mrs1-RNA holocomplex that reacts in an initial burst phase upon addition of the guanosine nucleotide (as illustrated in Figure 6A).

To measure equilibrium binding by the maturase to preformed Mrs1-RNA complexes, we formed complexes using trace concentrations of RNA and saturating concentrations of Mrs1. The fraction RNA bound by maturase is then reported as the fraction reacting in the burst phase of a splicing reaction (Figure 6A). The bI3 maturase binds to a preformed Mrs1-bI3 RNA complex with a K_D of 0.56 pM (circles in Figure 6B). Binding is 5-fold tighter than observed for interaction with the bI3 RNA alone as measured in a direct binding experiment (triangles in Figure 6B). Thus, there exists modest (1.0 kcal/mol) coupling between maturase and Mrs1 protein cofactors in assembly of the bI3 ribonucleoprotein (compare circles and triangles in Figure 6B).

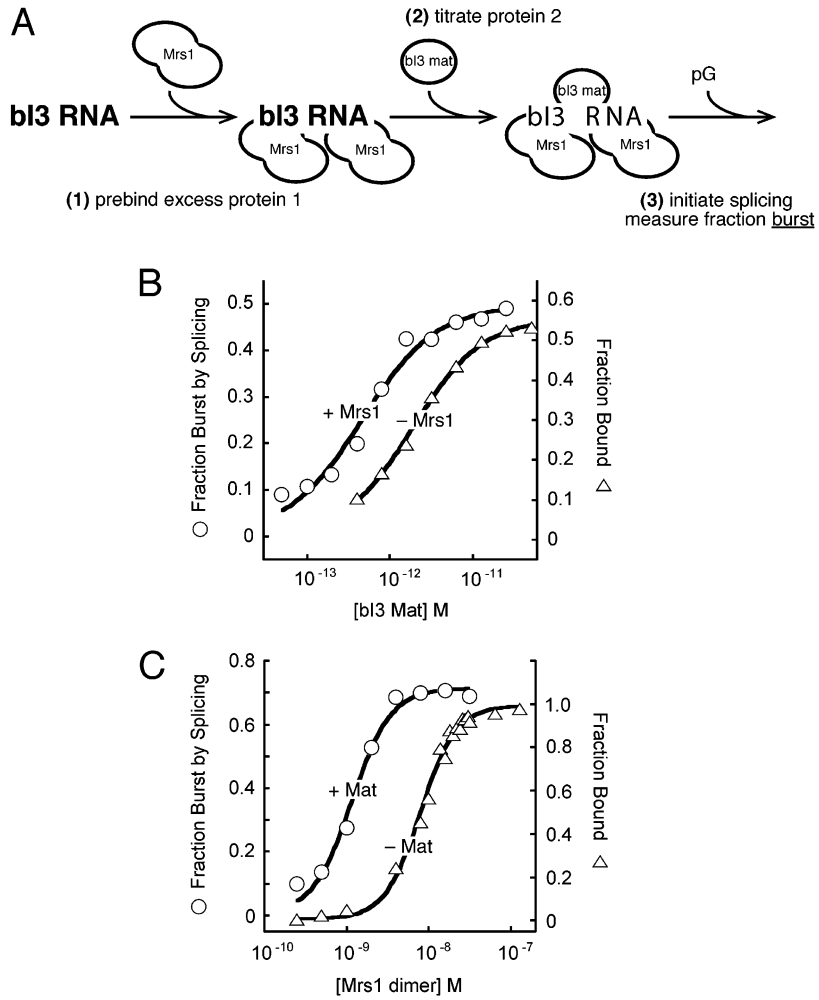

FIGURE 6: Interprotein coupling in the bI3 ribonucleoprotein holocomplex. (A) Monitoring protein binding in bI3 complexes via splicing. (1) Limiting concentrations of the bI3 RNA ($\ll K_D$) are prebound to excess protein 1 (either Mrs1 or bI3 maturase; Mrs1 binding is illustrated). (2) Protein 2 is titrated against protein 1−RNA complexes in separate splicing reactions. (3) The fraction of RNA precursor that splices in the first turnover reflects the fraction RNA bound by protein 2. (B) Maturase binding to free RNA and to preformed Mrs1−RNA complexes. Maturase binding to free RNA (triangles, −Mrs1) was measured directly (*3*) by filter partitioning; $K_D = 2.8$ pM. Binding to the Mrs1−RNA complex was monitored as the burst phase in a splicing experiment (circles); $K_D = 0.56$ pM. Curves are fit to an equation describing single-site binding: fraction bound or fraction burst $= m[\text{Mat}]/([\text{Mat}] + K_D)$, where m is the maximum fraction bound. (C) Mrs1 dimer binding to free RNA (ref *3*, −Mat, triangles) and to a preformed Mat-bI3 RNA complex (circles), monitored by direct binding or as the fraction burst in a splicing experiment, respectively. Curves are fit to an equation describing coupled binding: fraction bound $= m[\text{Mrs1}_2]^n/([\text{Mrs1}_2]^n + K_{1/2}{}^n)$, where n is the Hill coefficient. $K_{1/2}$ values for binding to the free RNA and to the maturase−RNA complex are 11 and 1.5 nM, respectively.

We used an analogous experiment to monitor binding by Mrs1 dimers to maturase−RNA complexes. Mrs1 binds the preformed maturase−RNA complex with a $K_{1/2}$ of 1.5 nM (circles in Figure 6C) or 7-fold more tightly (1.2 kcal/mol) than to the RNA alone (compare circles and triangles in Figure 6C). In both cases, binding by two Mrs1 dimers is strongly cooperative (Hill coefficient ≥ 1.8).

Placing Limits on the First and Second Mrs1 Dimer Binding Events. The molecular details of RNA binding by two Mrs1 dimers are strongly Mg^{2+} dependent (ref *3* and Figure 7B). Binding by Mrs1 dimers is strongly coupled at 20 mM Mg^{2+} and is uncoupled in the absence of divalent ion. Binding of a single (dimer) ligand at two independent sites is described as homotropic binding (*22*). The extent of binding for the mechanism shown in Figure 7A is

$$F = \frac{K_{D2}[\text{Mrs1}_2] + [\text{Mrs1}_2]^2}{K_{D1}K_{D2} + K_{D2}[\text{Mrs1}_2] + [\text{Mrs1}_2]^2} \qquad (1)$$

where F is the fraction RNA bound, and K_{D1} and K_{D2} are the equilibrium dissociation constants for the first and second Mrs1 dimer binding events, respectively. In noncooperative binding, K_{D1} can be smaller than (corresponding to tighter binding) or approximately equal to K_{D2}. For cooperative binding (Hill coefficient > 1), K_{D2} must be smaller than K_{D1}.

In principle, it is possible to obtain K_{D1} and K_{D2} by direct fitting of eq 1 to binding curves such as those shown in Figures 6C and 7B. In practice, obtaining unique values for the two equilibrium dissociation constants requires that the data be essentially without experimental error. In our approach, we used iterative fitting to eq 1 and visual inspection of calculated binding curves to either determine or place limits on K_{D1} and then define a relative affinity index, ρ, equal to K_{D2}/K_{D1} (Figure 7A,C). Values of ρ less than one thus correspond to cooperative RNA binding by Mrs1.

At 0 mM Mg^{2+}, the data are well-fit if the first Mrs1 dimer binds with a K_{D1} of 0.1 nM and the second Mrs1 dimer binds

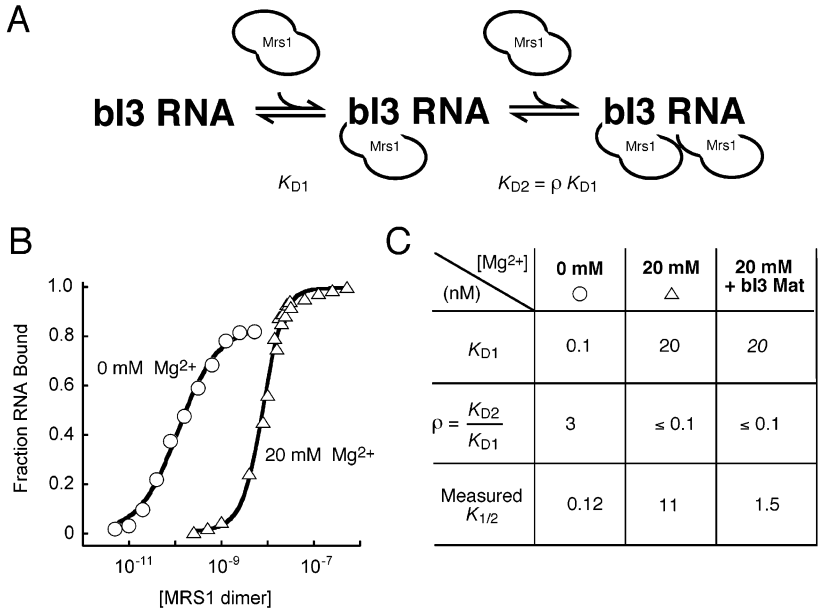

FIGURE 7: Placing limits on binding by the first and second Mrs1 dimers. (A) Scheme for analysis of the first and second Mrs1 dimer equilibrium dissociation constants. K_{D1} is estimated explicitly, and the relative affinity reflected by K_{D2} is reported as the ratio, ρ. Values of ρ less than one correspond to positive coupling. (B) RNA binding by Mrs1 at 0 mM (circles) and 20 mM (triangles) Mg^{2+} fit to eq 1. Data for this panel are reproduced from ref *3* and Figure 6C. (C) Individual binding constants estimated for 0 and 20 mM Mg^{2+} and for the holocomplex (20 mM Mg^{2+} + bI3 maturase; see Figure 6C).

with K_{D2} at least 3-fold greater than K_{D1}, $\rho \geq 3$ (Figure 7B, circles). The first Mrs1 dimer binding event is approximately equal to the observed $K_{1/2}$ of the Mrs1-bI3 RNA complex (Figure 7B,C).

At 20 mM Mg^{2+}, binding data are well-fit if K_{D1} is ≥20 nM and the second binding event, K_{D2}, is at least 10-fold tighter than K_{D1} [Figure 7B (triangles) and C]. Essentially identical behavior is observed for Mrs1 binding to the preformed bI3 maturase−RNA complex at 20 mM Mg^{2+} (Figure 6C). However, it is not possible to place tight limits on the strength of the first binding event because of greater experimental uncertainty for individual points in this binding curve (Figure 7C, italics). Under conditions optimal for splicing (20 mM Mg^{2+}), the first Mrs1 dimer thus binds relatively weakly to the RNA but generates a new environment with significantly higher affinity for the second Mrs1 dimer.

DISCUSSION

Assembly of the bI3 Group I Intron Ribonucleoprotein Catalyst. Our assembly framework for the bI3 group I intron ribonucleoprotein catalyst is outlined in Figure 1. Both bI3 maturase and Mrs1 proteins bind independently to the RNA to yield protein bound states bI3 RNA′ and bI3 RNA″, respectively. Neither the free RNA nor the RNA bound by either protein alone splices detectably in vitro. At 20 mM Mg^{2+}, two Mrs1 dimers bind cooperatively to the RNA. Binding by the first dimer creates a new interface (I in Figure 1) that strengthens binding by the second dimer by at least 10-fold (1.4 kcal/mol). Binding by Mrs1 dimers and by maturase is mutually positively coupled. Prior binding by one protein strengthens binding by the second protein by 5−7-fold (1.0−1.2 kcal/mol). The six-subunit bI3 holoribonucleoprotein is active in splicing reactions (italic bI3 RNA text in Figure 1).

The Michaelis constant, K_M, for guanosine monophosphate is consistent with the authentic binding step for this substrate (*3*) and is 0.2 mM. The rate of splicing by the holocomplex is 0.3 min^{-1} and significantly faster than dissociation of Mrs1 or bI3 maturase protein, either from the RNA alone or from the holocomplex. In the absence of other factors or processes that function to disrupt the complex, protein dissociation would limit subsequent splicing of additional bI3 group I intron-containing pre-mRNAs.

$k_{off}/k_{on} \neq K_D$ Kinetic Signature in Mrs1 Assembly. The calculated ratio, k_{off}/k_{on}, for cooperative binding by two Mrs1 dimers is at least 15-fold lower than the observed $K_{1/2}$. Disagreement between the ratio of dissociation to association rate constants, determined in a partitioning experiment, and an equilibrium K_D is a useful kinetic signature for formation of an obligate kinetic intermediate in a macromolecular assembly reaction (*2*, *21*). The apparent discrepancy arises because k_{on} and k_{off} report elementary steps at different transitions in the overall assembly pathway (*21*). A strong candidate for the required physical intermediate is the state, I (see Figure 1), in which the bI3 RNA is bound by the first of two Mrs1 dimers.

Analysis of Mrs1-RNA assembly in the absence of Mg^{2+} directly supports this model. At 0 mM Mg^{2+}, two Mrs1 dimers bind noncooperatively to the bI3 RNA, and the ratio k_{off}/k_{on} is approximately equal to the $K_{1/2}$ of 0.12 nM (see 0 mM Mg^{2+} reactions in Figure 1). Thus, while there still exists the physical intermediate, I, corresponding to binding by one Mrs1 dimer, the kinetics of formation and dissociation of the intermediate complex dominates the assembly reaction, and no discrepancy between k_{off}/k_{on} and $K_{1/2}$ is observed.

Analysis of Mrs1 assembly thus supports three strong conclusions. First, the obligate intermediate in Mrs1 assembly at 20 mM Mg^{2+} is the Mrs1-I state with one Mrs1 dimer bound to the RNA. These data also support assigning the observed k_{on} and k_{off} rate constants to pre- and post-

intermediate steps in coupled Mrs1 assembly. Thus, we assign k_{on} (1×10^8 M^{-1} min^{-1}) to formation of the Mrs1-I state and k_{off} (0.07 min^{-1}) to dissociation of the first Mrs1 dimer from the complex comprised of two Mrs1 dimers and the bI3 RNA (Figure 1). Second, because the second Mrs1 binding event changes from being ~3-fold weaker to at least 10-fold tighter than initial protein binding, the net effect of Mg^{2+} is to increase the relative binding affinity of the second Mrs1 dimer by at least 30-fold (2 kcal/mol). Finally, the bI3 RNA will exist predominantly in either the free state or in a fully bound (two Mrs1 dimers) state under conditions that support splicing.

bI3 Maturase Assembles with the bI3 RNA in a Single Kinetic Step: Contrast to Other Group I Intron Protein Cofactors. The bI3 maturase is an unusual group I intron protein cofator in that formation of the bimolecular protein−RNA complex is well-described by simple second-order kinetics. The bI3 maturase associates rapidly with and dissociates slowly from the bI3 RNA. The equilibrium K_D, 2.8 pM, is in excellent agreement with that calculated assuming a single step binding mechanism ($k_{off}/k_{on} = 1.9$ pM).

This single step binding contrasts sharply with the behavior observed for other well-studied proteins that form stoichiometric complexes with group I intron RNAs including CBP2 (*2*, *23*), CYT-18 (*2*, *24*), the AnCob LAGLIDADG-motif maturase (*11*, *13*), or Mrs1 (this paper). For each of these latter proteins, there exists an apparent discrepancy between the k_{off}/k_{on} ratio and the equilibrium K_D, indicating an obligate kinetically significant intermediate state in the assembly pathway (*21*).

Strikingly, the molecular basis for assembly intermediates for CBP2, CYT-18, and Mrs1 are distinct. Assembly of CBP2 is limited by a unimolecular RNA folding step (*2*, *23*); CYT-18 forms an active RNA−protein complex in its predominant assembly pathway only after proceeding through at least two intermediate states (*2*); and Mrs1 assembly involves a strongly linked binding event with a second Mrs1 dimer (Figures 6C and 7). A fourth cofactor protein, the AnCob maturase, shares 65% sequence identity (over the core maturase domain) with our bI3 maturase construct, yet appears to assemble with its cognate RNA via multiple kinetically significant steps (*11*, *13*). Thus, relatively small changes in the protein cofactor, RNA recognition site, or experimental conditions may have significant consequences for the molecular details of a ribonucleoprotein assembly reaction.

Protein−Protein Cooperativity Evident by Distinctive Mechanisms. RNA binding by both bI3 maturase and Mrs1 is enhanced 5−7- fold upon prior binding by the other protein (Figure 1). The physical basis for interprotein coupling is distinct for each component.

For the bI3 maturase, the rate constants for dissociation from either the free RNA or the holocomplex are identical. To account for the observed protein−protein coupling, we infer that prior binding by Mrs1 accelerates maturase binding. We showed that the association rate constant for maturase binding to the free RNA is equal to k_{off}/K_D. If we assume that this calculation holds true for binding to the Mrs1−RNA complex (meaning that no new intermediates are introduced), then the maturase binds to form the holocomplex at 3×10^{10} M^{-1} min^{-1} (value in parentheses in Figure 1). The maturase binds to a preformed Mrs1−RNA complex right at the diffusion-controlled limit.

Mrs1 binding to the bI3 RNA is strengthened 7-fold upon prior binding by the maturase. This favorable coupling increment is the same, within error, as the observed difference in k_{off} for dissociation of Mrs1 from the free RNA versus from the holocomplex. Thus, we infer that prior binding by maturase functions to slow dissociation of Mrs1 from the holocomplex.

In summary, there exists an approximately symmetrical, positively coupled, binding by maturase and Mrs1 (Figure 1). Prior binding by Mrs1 accelerates maturase binding (to the diffusion-controlled limit), whereas maturase binding slows dissociation of Mrs1 from the six-subunit complex.

Tight Binding but Moderate Coupling: Independent RNA Binding sites for Mrs1 and the bI3 Maturase. The bI3 maturase and Mrs1 play essential, independent roles in forming the RNA-based catalytic active site because splicing is only observed for the six-component holoribonucleoprotein and not for partially assembled complexes (*3*). Maturase and Mrs1 bind tightly in the holocomplex; K_D and $K_{1/2}$ are 2.8 pM and 1.5 nM, respectively. Maturase binding is among the highest affinity RNA−protein complexes. Despite the tight binding, interprotein coupling is modest, amounting to only ~1 kcal/mol. Tight binding, but modest coupling, between essential protein components supports a physical model in which both proteins interact at independent sites on the bI3 RNA, perhaps in distinct RNA domains.

Predominant bI3 Ribonucleoprotein Assembly and Dissolution Pathways. The overall assembly pathway will be governed by the relative concentrations of protein and RNA components and the underlying rate constants. In mitochondria, protein and RNA activities will be modulated by being sequestered into distinct mitochondrial regions, by the potential membrane localization of the bI3 maturase, by macromolecular crowding and the ion environment, and by adjunct factors or processes. Mrs1 also functions to facilitate splicing by the mitochondrial aI5β intron (*25*), which may alter its availability. Any proposal for a predominant assembly pathway hinges upon estimates for the effective concentration of each component.

Because the k_{on} for maturase is much larger than that for Mrs1 (Figure 1), the only scenario in which Mrs1 would bind first is if the effective concentrations of maturase and the intron are 70-fold lower than that for Mrs1 ($k_{on}^{Mat}/k_{on}^{Mrs1} = 70$). In contrast, if both proteins are present at near-stoichiometric effective concentrations or if either the maturase or RNA concentration were comparable to the Mrs1 concentration, maturase would usually bind first.

bI3 maturase dissociation from the free RNA versus from the holocomplex is unaffected by Mrs1 binding. In contrast, the dissociation rate constant for Mrs1 decreases, 5-fold, to that observed for the maturase. The 5-fold effect on k_{off} is comparable to the 7-fold favorable coupling of Mrs1 and maturase binding. These data are consistent with a model in which the rate determining step for holocomplex disassembly is dissociation of the bI3 maturase. Once the maturase dissociates, Mrs1 will then dissociate with k_{off} equal to 0.07 min^{-1} (see Figure 1).

The predominant assembly pathway for the bI3 ribonucleoprotein thus plausibly involves initial rapid, tight binding by the bI3 maturase, followed by a slower, but strongly

coupled, assembly by two Mrs1 dimers (top pathway in Figure 1). Disassembly, limited by maturase dissociation, would appear to occur in one step. Thus, relatively simple apparent pathways can emerge, even in cases where protein components interact independently with an RNA. Comparable principles are likely to underlie assembly and reorganization of more complex cellular ribonucleoproteins.

ACKNOWLEDGMENT

We thank Drs. Keith Bjornson and Jaga Lazowska for helpful discussions.

REFERENCES

1. Gesteland, R. F., Cech, T. R., and Atkins, J. F. (1999) *The RNA World*, 2nd ed., Cold Spring Harbor Laboratory, New York.
2. Webb, A. E., Rose, M. A., Westhof, E., and Weeks, K. M. (2001) *J. Mol. Biol. 309*, 1087−1100.
3. Bassi, G. S., de Oliveira, D. M., White, M. F., and Weeks, K. M. (2002) *Proc. Natl. Acad. Sci. U.S.A. 99*, 128−133.
4. Michel, F., and Westhof, E. (1990) *J. Mol. Biol. 216*, 585−610.
5. Golden, B. L., Gooding, A. R., Podell, E. R., and Cech, T. R. (1998) *Science 282*, 259−264.
6. Cech, T. R. (1990) *Annu. Rev. Biochem. 59*, 543−568.
7. Weeks, K. M., and Cech, T. R. (1995) *Biochemistry 34*, 7728−7738.
8. Weeks, K. M., and Cech, T. R. (1995) *Cell 82*, 221−230.
9. Myers, C. A., Wallweber, G. J., Rennard, R., Kemel, Y., Caprara, M. G., Mohr, G., and Lambowitz, A. M. (1996) *J. Mol. Biol. 262*, 87−104.
10. Caprara, M. G., Lehnert, V., Lambowitz, A. M., and Westhof, E. (1996) *Cell 87*, 1135−1145.
11. Ho, Y., and Waring, R. B. (1999) *J. Mol. Biol. 292*, 987−1001.
12. Geese, W. J., and Waring, R. B. (2001) *J. Mol. Biol. 308*, 609−622.
13. Solem, A., Chatterjee, P., and Caprara, M. G. (2002) *RNA 8*, 412−425.
14. Lazowska, J., Claisse, M., Gargouri, A., Kotylak, Z., Spyridakis, A., and Slonimski, P. P. (1989) *J. Mol. Biol. 205*, 275−289.
15. Dalgaard, J. Z., Klar, A. J., Moser, M. J., Holley, W. R., Chatterjee, A., and Mian, I. S. (1997) *Nucl. Acids Res. 25*, 4626−4638.
16. Ho, Y., Kim, S. J., and Waring, R. B. (1997) *Proc. Natl. Acad. Sci. U.S.A. 94*, 8994−8999.
17. Lilley, D. M. J., and White, M. F. (2000) *Proc. Natl. Acad. Sci. U.S.A. 97*, 9351−9353.
18. Gill, S. C., and von Hippel, P. H. (1989) *Anal. Biochem. 182*, 319−326.
19. Beebe, J. A., and Fierke, C. A. (1994) *Biochemistry 33*, 10294−10304.
20. Gutfreund, H. (1995) *Kinetics in the Life Sciences: Receptors, Transmitters and Catalysts*, pp 270−275, Cambridge University Press, Cambridge, UK.
21. Rose, M. A., and Weeks, K. M. (2001) *Nature Struct. Biol. 8*, 515−520.
22. Wyman, J., and Gill, J. S. (1990) *Binding and Linkage: Functional Chemistry of Biological Macromolecules*, pp 4−9 and 39−41, University Science Books, Mill Valley, CA.
23. Weeks, K. M., and Cech, T. R. (1996) *Science 271*, 345−348.
24. Saldanha, R. J., Patel, S. S., Surendran, R., Lee, J. C., and Lambowitz, A. M. (1995) *Biochemistry 34*, 1275−1287.
25. Bousquet, I., Dujardin, G., Poyton, R. O., and Slonimski, P. P. (1990) *Curr. Genet. 18*, 117−124.

BI0346906